Journal of Atmosphere
2025 Vol. 8, No. 1, pp. 1-18
ISSN(e): 2414-2484
ISSN(p): 2518-2528
DOI: 10.18488/94.v8i1.4653

Nitrogen oxides and NO_2 primary composition in earth's atmosphere

Kole Lutz
MPU University, Washington DC, United States.
Email: kole@mp-university.net

Article History
Received: 7 October 2025
Revised: 9 December 2025
Accepted: 22 December 2025
Published: 31 December 2025

Keywords
Atmosphere sciences
Climate change
Earth sciences
Planetary science.

ABSTRACT

Humans believed Earth was 78% nitrogen (N_2) and 21% oxygen (O_2) until the 2020s. Based on data collected by balloons and satellites since the 1980s, evidence suggests that Earth's atmosphere is composed of complex molecules such as nitrogen dioxide (NO_2) with polar bent molecular structures, similar to water (H_2O). Although nitrogen-oxygen mixing ratios have been recorded for over 50 years, they have often been overlooked in studies of redox reactions, biological systems, and nitrogen-fixing bacteria. Microorganisms, including bacteria in oceans and soils, release nitrous oxides, NO_2, NO, and N_2O, which are abundant in these environments. Nitric oxide (NO) is also among the most prevalent molecules in biological systems; experiments indicate that NO_2 and NO diffuse rapidly across cell membranes. Measurements at altitudes of 10-12 km show a ratio of 1 NO to 2-6 times NO_2, with air density estimates indicating 300-400% more NO_2 compared to NO at the surface. Near the surface, the ratio is approximately $_2$:1 NO, similar to the historically accepted 78% nitrogen measurements. This data suggests that the air density of NO_2 is less than 2.05257 g/L or kg/m^3, which is about 68% heavier than the standard air density of 1.19 g/L. Ongoing research enhances data models related to atmospheric composition, aerodynamics, climate change, biological processes, materials science, surface redox reactions, and planetary studies.

Contribution/Originality: This study contributes to the literature by introducing new insights into atmospheric sciences and composition. It enhances understanding of data, chemistry, and models related to atmospheres, aerodynamic systems, climate change, biological systems, materials, surface redox reactions, and planetary sciences.

1. INTRODUCTION

Nitrogen has been overlooked in air molecules, chemistry, and reactions for centuries, as oxygen was overemphasized. Nitrogen (N_2) was discovered by Rutherford by removing oxygen from CO_2 in an enclosed environment with a candle in 1772. After burning phosphorus inside a container and placing a mouse inside, many questioned how the mouse died. Once the CO_2 was removed and the candle fire waned, Rutherford called the remaining noxious or phlogisticated air, which was later assumed to be nitrogen. However, questions remained regarding the selectivity and measurement accuracy of current tools used to quantify remaining molecular compounds. Shortly afterward, Priestly discovered oxygen by heating mercury O-Hg-O or mercury nitrate (pyrolysis of $Hg(NO_3)_2$) in 1774 and the late 1770s. By focusing sunlight with glass, combustion or molecular dissociation produces mercury (II) oxide (HgO), nitrogen dioxide (NO_2), and oxygen (O_2). In 1772, Henry Cavendish conducted experiments [1] in which he passed air over heated coals, claiming to 'remove oxygen' and isolate 'nitrogen,' which he referred to as phlogisticated air. His experiments revealed a ratio of approximately 4:1, although this was later interpreted as predominantly nitrogen. These ratios are consistent with nitrogen oxide mixing ratio measurements collected in the 2020s.

1.1. Earth Nitrogen Cycle on Land and Oceans

Some propose that nitrogen originated from comets impacting Earth. Labidi et al. [2] employed a technique to remove air from gases in order to determine the proportion of nitrogen (N15/N14) derived from air in volcanic emissions.

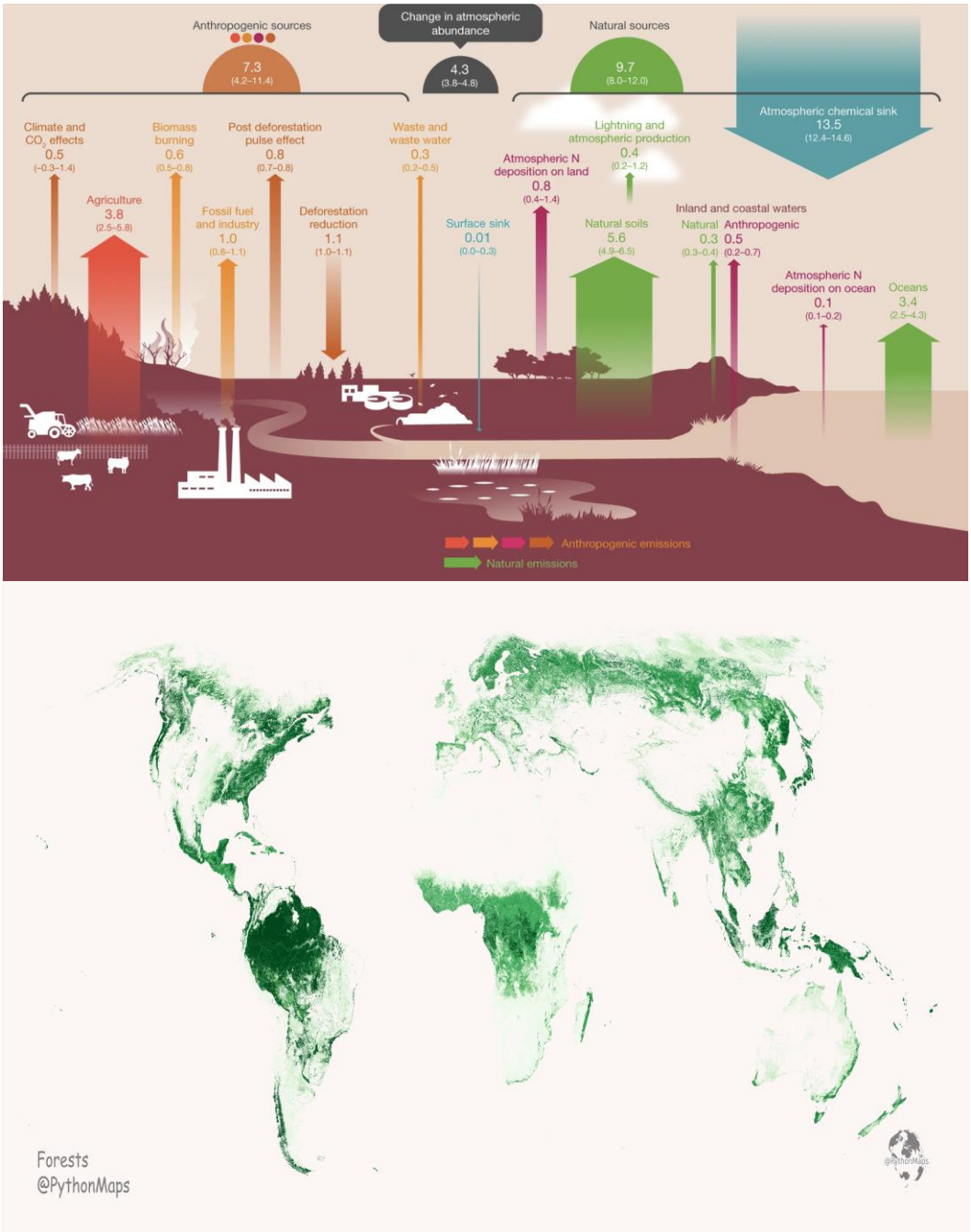

Figure 1. Nitrous oxide fluxes (in Tg N yr−1 for 2007–2016) with uncertainty in Nitrous oxide budget, b) 10-year average Nitrous oxide emissions from land and ocean and c) Earth Forests from PythonMaps [2].

Volcanoes release nitrogen dioxide (NO_2), as well as nitrate (NO_3) and HNO_3. Near-source plumes were measured from four volcanoes in Nicaragua, Italy, and Chile. Data suggest that a significant fraction of NO may be oxidized to form NO_2 and NO_3^- over several hours. Volcanic plume concentrations of HNO_3 range from 1.8 to 5.6 μmol m^{-3}, representing an enrichment of one to two orders of magnitude over background levels (0.1–1.5 μmol m^{-3}). Models estimate the potential global flux of NO at approximately 0.02 Tg (N) per year and the flux of HNO_3 at around 0.02–0.06 Tg (N) per year [3].

Sánchez-Gutiérrez, et al. [4] used a CWFT tube reactor coupled with a blue light nitrogen oxides analyzer (NOx analyzer) to monitor in real time concentrations of NO2, NO, and HONO with Iceland volcano particles. Greater concentrations of NO_3- (up to approximately 63 mg/L) were reported in wells located at mid- and low-elevation sites on the volcano near Costa Rica over a four-year period. This trend suggests an increase in groundwater nitrogen levels in the area [4].

Considering NO mixing ratios (0.78N to 0.21O), nitrogen forms nine molecular oxides, some of which were among the first gases to be identified: NO_2, NO_3, N_2O, N_2O_3, N_2O_4, and N_2O_5. Approximately 99.63% of naturally occurring nitrogen is N_{14}, with the remaining being N_{15}. While some claim that NO_2 and N_2O are reactive, toxic gases associated with burning fossil fuels and other materials, both gases are common in Earth's atmosphere and are stable at room temperature. Plants also produce nitrous oxide during nitrate assimilation and denitrification, absorbing and utilizing both NO_2 and NO. In the early 1900s, Einstein mentioned how the proposed Haber-Bosch synthesis of ammonia (NH_3) involves pulling oxygen or nitrogen out of the air. A comparison of six atmospheric models with aircraft observations over the Pacific and Atlantic Oceans during the NASA Atmospheric Tomography Mission (ATom) campaign (July–August 2016) revealed a significant underestimation of NO in all models below 4 km in the tropics and subtropics [5]. Other studies also suggest a missing source of NOx in models over subtropical oceans from fast photolysis of nitrate [6-9] or from oceanic emissions [10].

$$P_h = P_0\, e^{(-mgh/kT)}$$

P is the pressure at height (h), and P_0 is the sea level pressure. The variable m represents the mass of molecule(s). The Mixing Ratio (w) is defined as follows:

$$w = m_\upsilon / m_a$$

$$w = n_\upsilon M_\upsilon / n_a M_a$$

The mixing ratio (w) of moist air, which consists of dry air and water vapor, is defined as the ratio of the mass of water vapor (m_v) to the mass of dry air (m_a). The molecular mass of water vapor (m_v) is 18.016 g/mol, while the molecular mass of dry air (m_a) is 28.966 g/mol. The typical value of the mixing ratio is approximately 0.622.

$$w_s \equiv m_{vs} / m_d$$

Saturation mixing ratio (w_s) is the ratio of the mass of water vapor to the mass of dry air, expressed in grams or kilograms. The saturation mixing ratio with respect to water is defined as the ratio of the mass m_{vs} of water vapor in a given volume of air that is saturated with respect to a plane surface of pure water to the mass m_d of dry air [11]. By measuring RH, it is possible to calculate the MR. Specifically, when the saturation vapor pressure $e_{sat}(t)$ is computed, the saturation value MR_{sat} can be obtained, and the actual MR can be determined accordingly.

$$MR = RH \times MR_{sat}$$

2. METHODS

This study outlines atmospheric chemistry reaction pathways involving NO, NO_2, HNO_3, and NO enthalpy mixing chemistry, ocean-atmosphere surface reactions, and spectral analysis, including vibration modes of polar bent molecular structures. A Nitrogen Bond Dissociation Energy analysis evaluates the energy requirements for molecules to break N_2 bonds. The study discusses global sources of nitrogen oxides, both natural and anthropogenic, from 21 sectors between 1980 and 2016, with 43 flux estimates. A detailed analysis of nitrogen oxide atmospheric composition describes vertical distributions, mixing ratios, and data measurements obtained from flight instruments and atmospheric source observations. The absorption modes of nitrogen oxides, including O_2, are outlined using spectroscopy methods in infrared and optical regions. The absorption spectra of NO and NO_2 gases, along with potential sources of variance, are analyzed to understand their behavior and impact in the atmosphere.

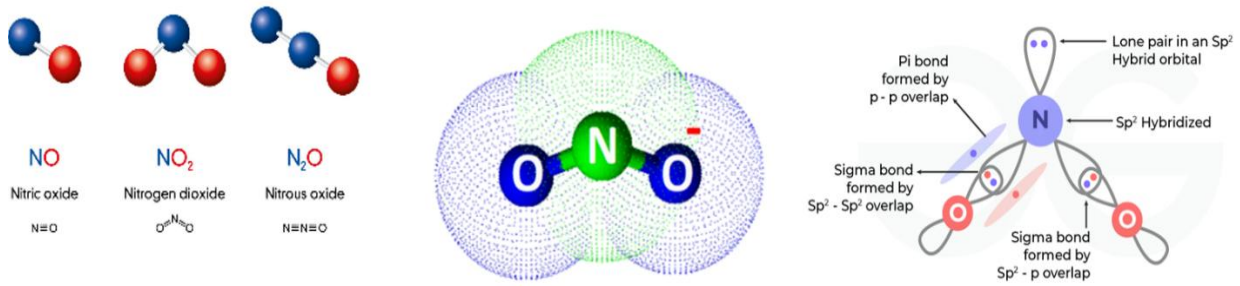

Figure 2. Nitrogen oxide molecules structures.

3. DATA AND RESULTS

3.1. Nitrogen Oxides Molecular Structures, Reaction Pathways

NO_2 is a polar molecule with a lone pair of electrons on N, resulting in a bent structure, similar to H_2O and CO_2. NO_2 has a molar mass of 46.005 g/mol, with an estimated bond angle of 115-134°, characterized by bending scissoring frequency and a dipole moment aligned with oxygen vibrations. NO_2^- also contains an extra electron, which may suggest a larger bond angle. Sigma bonds are more energetic than pi bonds but are believed to be stronger. The zigzag pattern as a function of orbital velocity, particularly in in-plane bending, suggests more common vibration modes. The average kinetic energy (KE) is estimated at 3/2Kb(t), but the KE of atoms and molecules may be a time series sum of electron quanta clusters and interactions. Although vibration modes can portray false representations of orbital velocity, the directions of molecular angular velocity and electric/magnetic fields are correlated with higher vibration mode energy ratios.

Nitrogen has 5 valence electrons based on $1s^2\ 2s^2\ 2p^3$, although this also depends on charge state. Both fewer valence electrons and N_2 would suggest greater reactivity to complete electron clouds. The reaction below indicates a lower energy barrier to form NO, which is a building block for compounds.

$$N_2 + O_2 \rightarrow NO + NO\ \Delta H° = +181 kJ/mol$$

$$2NO + O_2 \rightarrow 2NO_2\ \Delta H° = +6.47\ kJ/mol$$

$$N_2(g) + 2O_2(g) \rightarrow 2NO_2(g)\ \ \Delta H° = +431\ kJ/mol$$

$$2NO_2(g) \rightarrow 2NO(g) + O_2(g)\ \ \Delta H° = +114.2 kJ/mol$$

Some claim N_2 bonds need to be partially broken. To break N_2 bonds, an estimated minimum of 365 kJ/mol is required to break a single N_2 bond, with an additional +66.4 kJ to react with O_2 based on rough mathematical models. This suggests a less favorable reaction pathway in nitrogen-oxygen mixing gradients, toward reactions with lower kJ/mol values. The reaction $N_2 + O_2 \rightarrow 2NO$ was also previously proposed as endothermic and less spontaneous; however, the reactions below may indicate more favorable pathways.

$$N(g) + O(g) \rightarrow NO(g)\ \Delta H° = +90.25\ kJ/mol$$

$$2NO + O_2 \rightarrow 2NO_2\ \Delta H° = -112\ kJ/mol$$

NO is observed to have greater reactivity. N–O is a preferred bond arrangement to maintain reactivity and polar charge states, whereas O_2 and N_2 would have more complete valence electron shells, suggesting less reactivity. With lower $\Delta H°$, N–O or O–N is more reactive to fill valence electron clouds. While negative ΔG indicates a spontaneous reaction, $\Delta H°$ is also a function of electrons, charge states, and column mixing gradients.

Moreover, catalytic converters in cars were believed to form $O_2 + N_2$ and catalytic converter intake (HC, CO, NOx) and output (CO_2, N_2, O_2) based on information available on the internet. However, after high-temperature oxidation (HTO), which strips electron charge states, research suggests that N, O, and oxides would react to form metal oxides such as (Pl_nO, Pl_nN_n; Fe_nO, Fe_nN_n, Al_nO, Al_nN_n, etc.). NO_x-oxides would also be more prevalent in emissions with molecular compounds such as $NO_2H_2O_n$, NO_2Al, NO_2CO_{2x}, O_2CNO^-, etc., with varying vibration mode absorption bands.

In water or above the ocean surface boundary layer, nitric oxide reacts with oxygen to form nitrous acid (HNO_2) and nitrous acid (HONO) via the following reactions.

$$4NO + O_2 + 2H_2O \rightarrow 4\ HNO_2$$

$$NO + H_2O \rightarrow HNO_2 + H$$

HNO_2 is a key precursor to the formation of hydroxyl radicals (OH) in the atmosphere, which are important for binding to and removing pollutants and air metals. Updated ocean-atmosphere surface reactions play a crucial role in atmospheric and ocean chemistry. With negatively charged sink sources of Negative Air Ions (NAIs) from water, plants, and lightning, additional electrons fill valence shells. Lightning induces molecular dissociation of diatomic molecules such as NO, NO_2, O_3, HNO_3, and oxides. After orthogonal scattering of high charge state ions, electron scattering particle fluxes form reaction pathways and recombine to produce NO, NO_2, HNO_3, $NO_x \bullet H_2O$, etc.

$$NO_2 + OH \text{ -> } HNO_3$$

$$2NO_2 + H_2O \rightarrow HNO_3 + NO$$

Moreover, NO_2- (Nitrite) can react with CO_2 to form intermediates and potentially decompose to form OCO and nitrite. NO-CO reaction is important in various applications, such as three-way catalysts (TWCs) in vehicles CO_2- + NO → O_2CNO-.

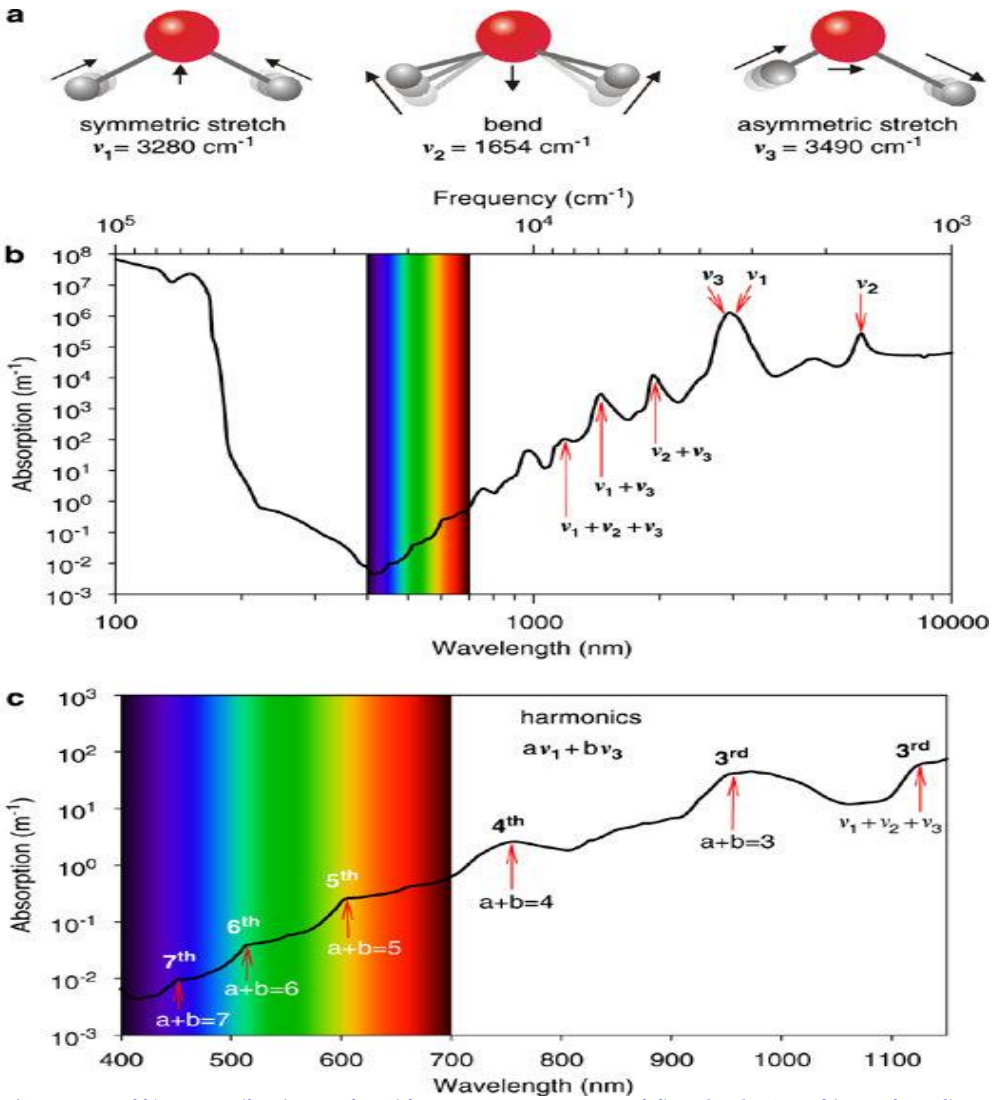

Figure 3. a and b) Water Vibration Modes with Raman Spectroscopy, and d) Molecular Stretching and Bending.

With proposed vibration modes correlated with energy, vibration modes may portray misrepresentation of how electron quanta clusters orbit in similar orbital velocity directions. If less common stretching events and closer to 130-180° angle between oxygen or atoms, stretching events would be correlated to movement of electron dE to lower energy shell to fill valence pair and/or bonding/mixing with other atoms and electrons, which could be observed distinguishably in spectra.

Data suggests atmospheres and planets have a preference for polar bent molecular structures. As H_2O provides preferred molecular pathways for denser atmospheres and cells, bent configuration of H_2O 104-109.5°. Some claim CO_2 is linear; others suggest rotation and vibration cause the effective (or average) structure of CO_2 to be bent, which is similar for any triatomic molecule [12]. While Raman relies on the deformation of electron clouds and is usually used for inorganic compounds, vibrational spectroscopy is an analytical method for in-situ monitoring of electrochemical reactions. With more extensive spectral databases, Fourier-transform infrared (FTIR) spectroscopy measures the absorption of IR wavelengths and changes in molecular dipole moments during vibrations. It is more sensitive to H2O and produces stronger signals; therefore, FTIR was used with LEC cells instead of organic OLEDs [13] and is accurate for measuring air molecules and nitrogen oxides [14].

3.2. Nitrogen Bond Dissociation Energy Analysis

Dinitrogen can be less reactive due to the triple covalent bond. To break N_2 bonds, 365 kJ/mol is estimated for the single bond, 598 kJ/mol for the double bond, and 813 kJ/mol is required for the triple bond, which can be assumed as rough approximates with many factors affecting dkJ/mol. The energy to break one mole of C-N bonds is 305 kJ/mol. Assuming an average of 813 kJ/mol for a cell to split N_2 triple bond, 813 kJ/mol would be recoverable if NO or NO_2 bonds are preferred. If the ideal gas law at 25°C and 1 atm suggests 2.46×10^{19} molecules in 1 cm^3 of air, then a 7.5 μm average cell radius with approximately 1767 μm^3 cubic volume per human cell, flux integration, diffusion models, nitrogen oxygen-carrying capacity rates, transportation, and related models would be updated accordingly. If NO molecules are more readily available, they could serve as molecules for hydrocarbons and amino acids, with NO bonds potentially recovering 813 kJ/mol of cellular energy or ATP. In NO_2, the bond dissociation energy of the N-O bond is 469 kJ/mol, which suggests that NO_2 provides lower energy pathways—about 57% less energy (469/813 kJ/mol) than N_2.

The free energy in a cell equation $\Delta G^0 = -nFE_{cell} = -96.5nE_{cell}$ is a time series of ATP produced from the mitochondria electron transport chain (ETC) from moving electrons with F = Faraday's constant = 96,500 C/mol e- or 96.5 kJ/mol e- V to get ΔG in kJ/mol, which suggests $\Delta G^0 = -96.5nE_{cell}$. As cells get energy from ATP ⇌ ADP + Pi, $\Delta G^0 = -33$ kJ/mol. Research suggests biological, cellular, and subcellular pathways achieve activation energy in hydrodynamic environments to form nitrogen oxides and to supply nitrogenous base pairs in DNA, amino acids, and proteins for life.

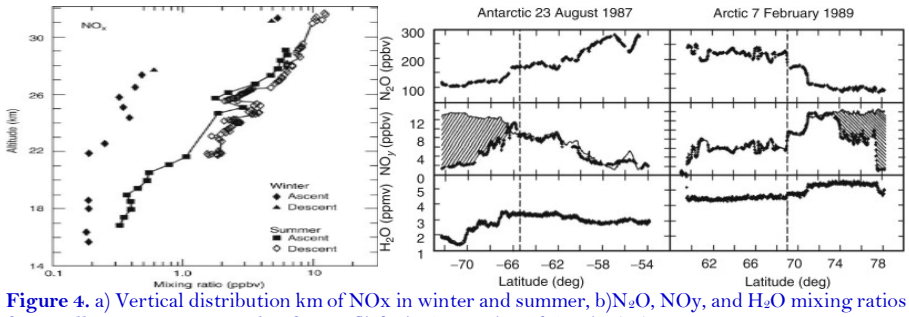

Figure 4. a) Vertical distribution km of NOx in winter and summer, b)N_2O, NOy, and H_2O mixing ratios from Balloon ER-2 at 16–19 km from a flight in Antarctic and Arctic [15].

3.3. Nitrogen Oxide Atmosphere Composition Analysis

NOx mixing ratios and NOx/NOy ratios have been observed to decrease sharply at latitudes higher than 50–60° in winter and early spring, as shown in Figure 12. These observations are based on balloon flight data collected around 51° N in 1982. Ridley et al. [16]. The shaded areas represent differences between measured NOy and NOy calculated from the equation, indicating denitrification pathways. Data collected with humidity mixing ratio (HMR) sensors suggest that trimolecular compounds are up to 30-200 times more abundant than NO. In background data around 12-15 km above the Arctic, NO is enhanced by a factor of 5-10 times, which is attributed to elevated temperatures and solar flux causing evaporation of HNO3–H2O condensation [15].

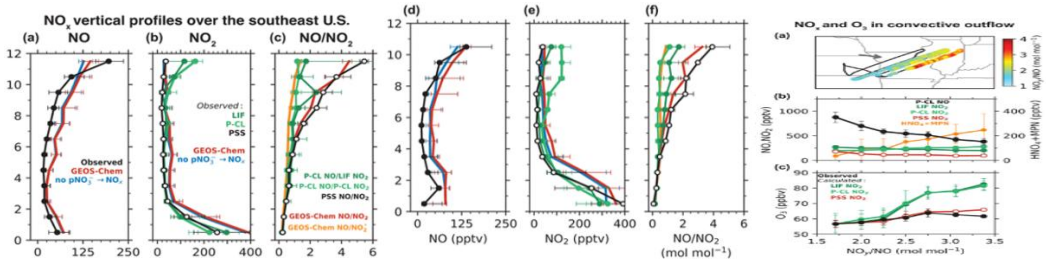

Figure 5. a) Vertical Columns Altitude (km) of observed and GEOS-Chem simulated NO and NO_2 from SEAC RS Campaign b) NO_x Data from DC3 Aircraft Campaigns [17], and c) NO_x & O_3 Outflows.

Three aircraft campaigns (SEAC4RS, DC3, and ATom) and four atmospheric chemistry models (GEOS-Chem, GMI, TM5, and CAMS) evaluate NO_2 with increased concentrations above 10 km in summer. GEOS-Chem reproduces the geometry of NO_2 in the troposphere but may overestimate NO_2 and underestimate nitration and NOx chemistry. The median PSS-inferred tropospheric NO_2 column density for the ATom campaign is $1.7 \pm 0.44 \times 10^{14}$ molecules/cm², and the NO_2 column density simulated by the four models ranges from 1.4 to 2.4 $\times$ 10^{14} molecules/cm², with an uncertainty of 1E14 molecules. Tropospheric NO_2 columns observed by satellites over the contiguous U.S. increase from $25 \pm 11\%$ in winter to $65 \pm 9\%$ in summer [17], which may be correlated with Negative Air Ions (NAIs). Tropospheric NO_2 does not vary significantly at regional scales, and finer-resolution tests showed similar results [18] with a spin-up period for model simulations of around six months. Moreover, Deep Convective Clouds and Chemistry (DC3) campaigns over the southeastern U.S. in 2012 measured midlatitude convective clouds with the NASA DC-8, NSF/NCAR Gulfstream-V, and ground radar networks, which were consistent with NO measurements. During campaigns, N_2 molecules were not documented. Between 10-12 km, NO: NO_2 ratios using LIF measurements are in the range of 1 to 2, while the PSS NO: NO_2 ratios are in the range of 3 to 6 from Shah et al. [17]. As models and several underestimate NO over the Pacific and Atlantic, and several researchers ponder nitrogen sinks over oceans, algae and lightning sources could provide NO_2:NO mixing pathways.

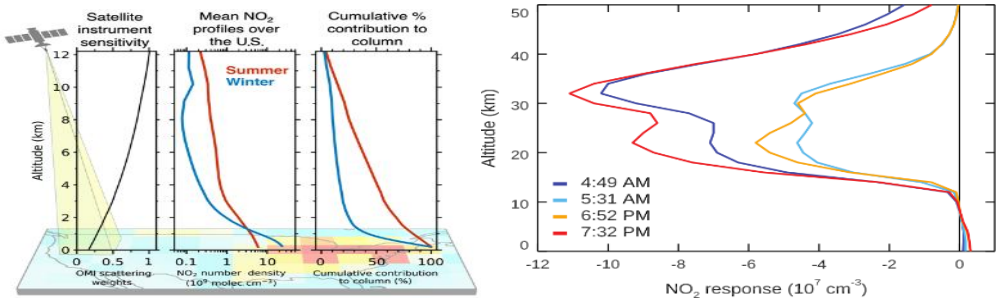

Figure 6. NO_2 Number Density and Vertical Columns %, and sensitivity (scattering weights) of the OMI satellite instrument, suggesting >10E9-10 NO_2 /cm^3 [17] and b) Changes in NO_2 number density.

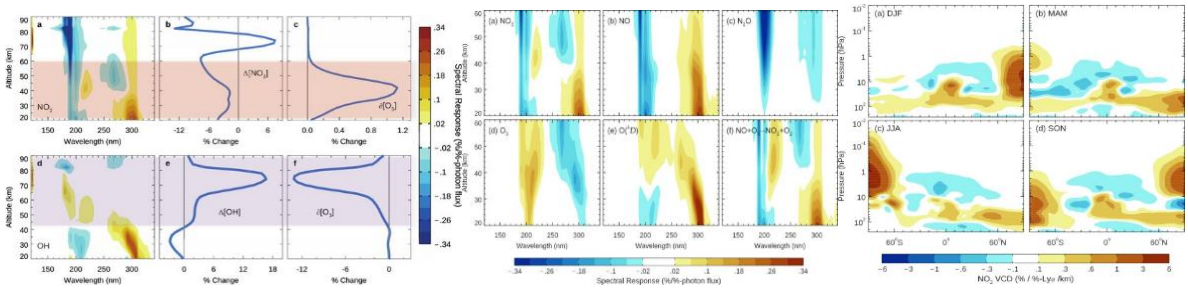

Figure 7. a) NO_2 response (% change in NO2) to changes in solar UV irradiance (% change in the photon flux). (b) Vertical profiles of NO_2 solar-cycle signal from the model. and c) CCMI WACCM SD model run from 1979 to 2014. The NO_2 solar-cycle response in each of the four seasons [19].

NO_2 vertical column density (VCD) data from NDACC, collected at 16 stations during Solar Cycles 23 and 24, suggests high variability in NO_2. The solar-cycle variability of NO_2 is believed to play a vital role in regulating ozone (O_3) at altitudes of 20-60 km, while the variability of hydroxyl radicals (OH) influences ozone levels at 40-90 km [19]. Moreover, satellite instruments are more sensitive to NO_2 in the troposphere, which could be due to atmospheric scattering versus atmospheric boundary layer (ABL), the lowest part of the atmosphere, typically within

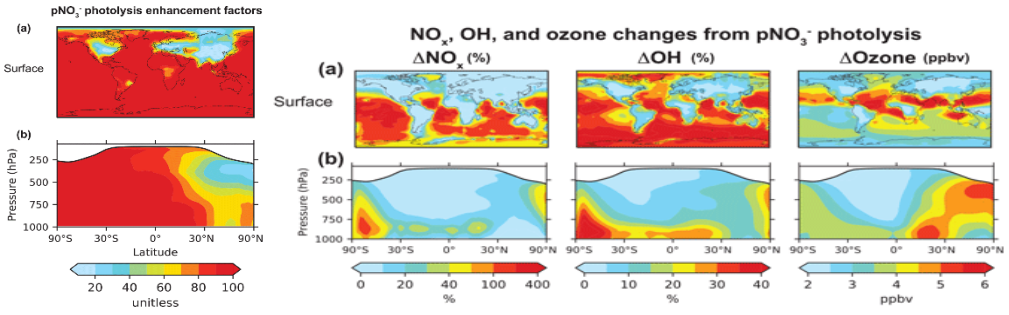

Figure 8. Annual (2015) enhancement factors (EFs) for the photolysis frequency of pNO3- and b) Annual mean (2015) changes in NOx, OH, ozone from pNO_x photolysis in GEOS-Chem [17].

Data suggests lightning is the main NOx source over the tropics and southern midlatitudes and over the U.S. in the summer, contributing 62%–73% of the NOx columns in the free troposphere. Higher free tropospheric NO_2 columns in summer are due to lightning emissions and increased light/photons [17]. Simulated NO_2 partial columns in the boundary layer and the free troposphere are 6.9×10^{14} and 5.8×10^{14} molecules/cm^2. Simulated wintertime NO_2 partial columns are 15.4×10^{14} in the boundary layer and 1.9×10^{14} molecules/cm^2 in the troposphere.

NOAA data and animation show a time series of NO_2 measured from satellites from October 2004 to December 2009. In the northern hemisphere winter, peak NO_2 levels are higher in all northern hemisphere hotspots [20]. Urban centres are correlated with 'NO_2' regions, which correspond to areas with high populations. However, imaging vibration bands and mixing ratios from satellites pose a challenge in distinguishing between NO_2 and $NO_2.Al_n$, NO_2, Pb_n, NO_2, Cd_nO_n.

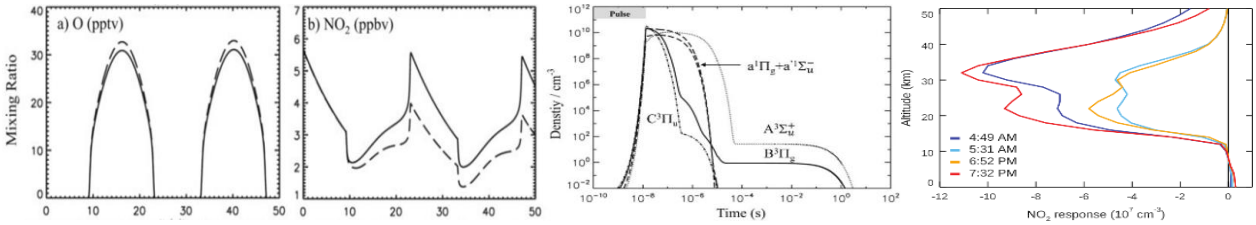

Figure 9. a) volume mixing ratio of (a) atomic oxygen, (b) NO2, and c) excited N2 or molecular nitrogen species at 27 km when streamer pulse occurs [21].

Some suggest 2.7 x 10^{19} molecules in every cm^3 of air, although other data suggest 10^{E10} molecules/cm^3. Previous data from Shah suggest NO_2 partial columns are estimated between 6.9×10^{14} and 5.8×10^{14} molecules/cm^2 simulated. This would suggest 83,066,238 molecules/cm and 5.73×10^{22} molecules/cm^3 of NO_2. Given the limitations of instrument, sensor, and detector accuracies, further R&D is necessary to better quantify molecules per cm^3 of air.

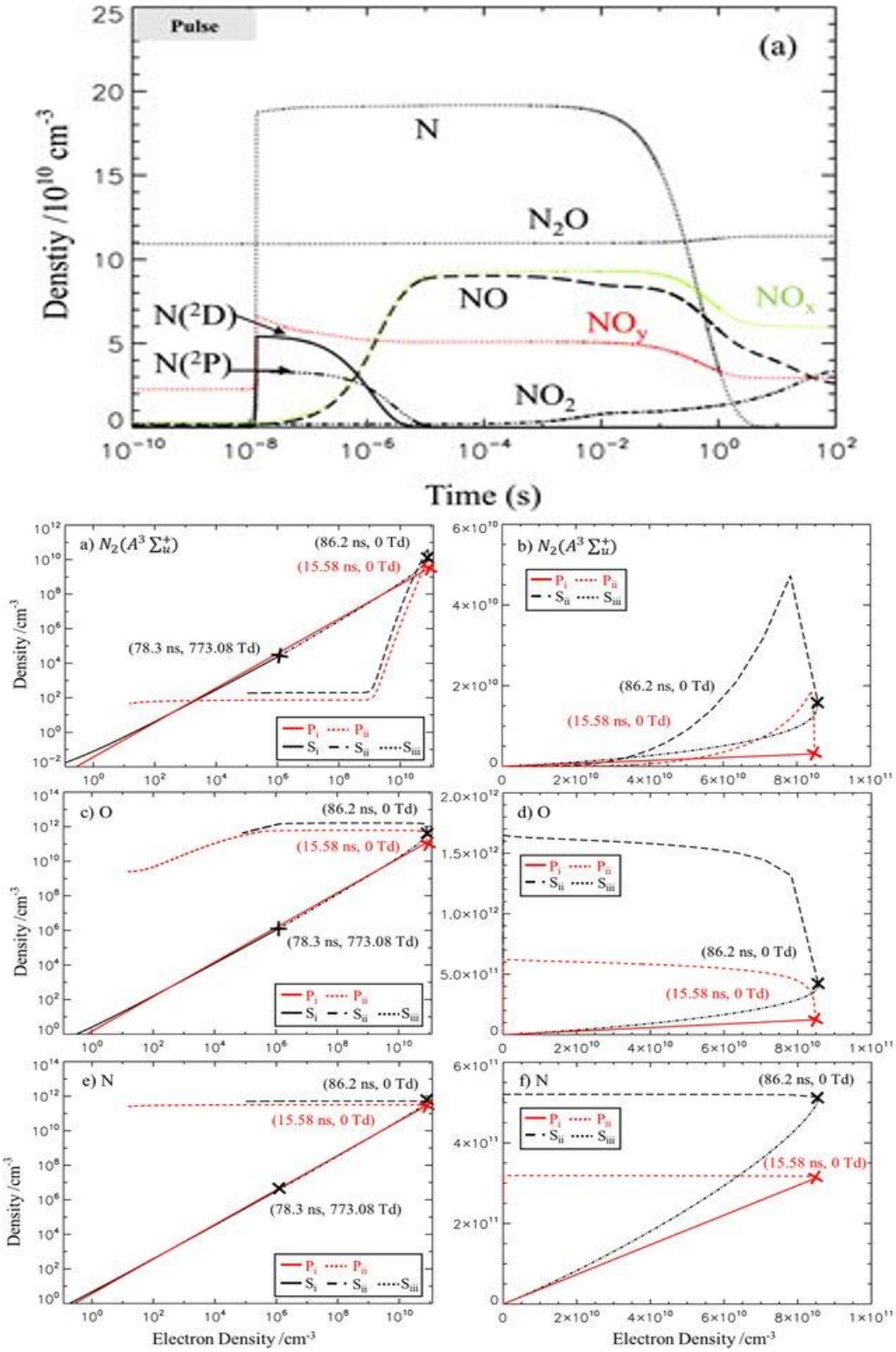

Figure 10. a) Time evolution of Charged Nitrogen species at 27 km when streamer pulse occurs, b) Density correlations between N2A3∑u+, atomic oxygen and nitrogen to electron. derived from electro dynamic simulations (b,d,f in linear scale) where crosses are transitions of E-field stages [21].

As used in W2015, the electric field is measured with a simple boxcar field after the sensor passes the streamer tip to measure electron density fluctuations. Simulations are also performed during daytime/nighttime and in two-day long-term durations at 27 km [21]. With varying start/end locations of nitrogen curves (NO, NO_2, NO_x), N_2 and N_2O curves appear dissimilar from regression data fits. Future R&D may quantify similarities between absorption lines of N_2 that may be correlated with N_2O, NO_2, etc.

3.4. Nitrogen Oxides, O_2 Absorption Modes with IRRAS Infrared Spectroscopy

As a technique of IR FTIR spectroscopy, Infrared Reflection Absorption Spectroscopy (IRRAS) measures molecules adsorbed on surfaces, thin films, or reflective layers with IR reflectance at a grazing incidence angle, or also as RAIRS (Reflection Absorption Infrared Spectroscopy). IRRAS can measure other gases with IR absorption bands, considering molecular scattering direction and velocity.

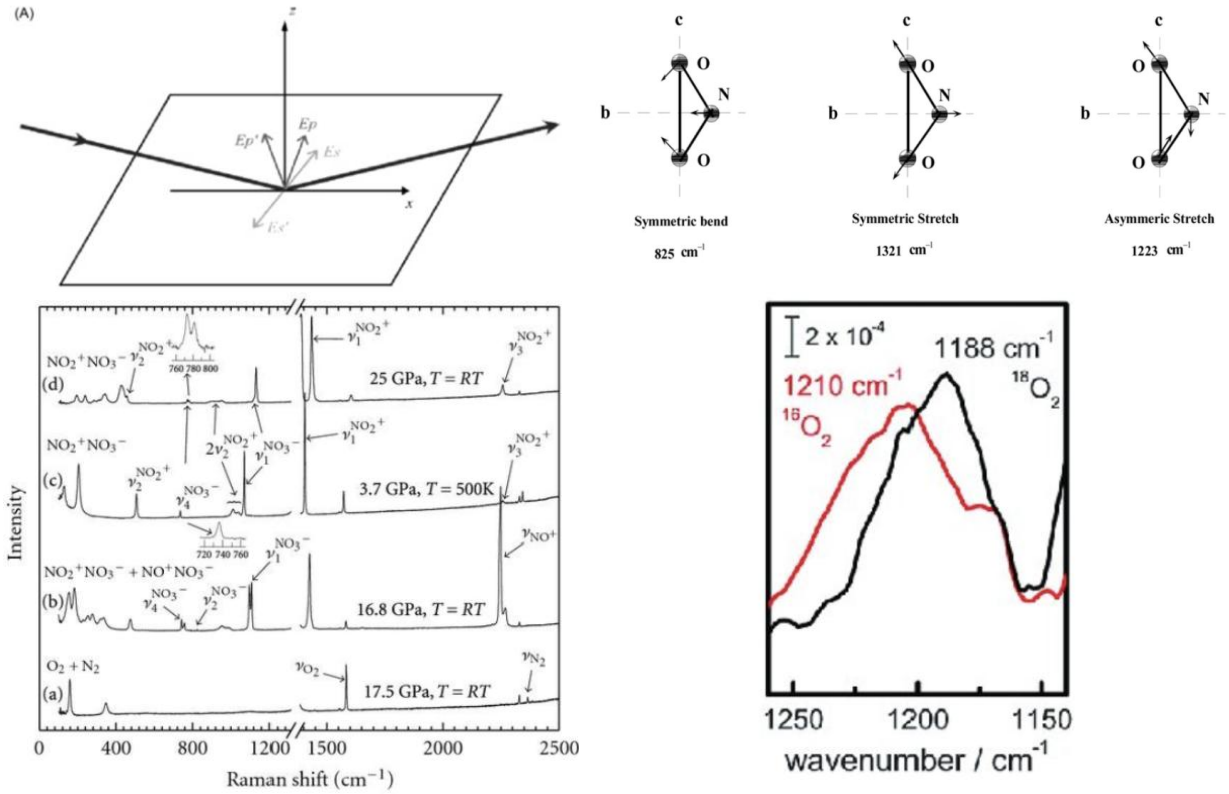

Figure 11. a) IRRAS Geometry, b) Internal modes of NO_2^- taken from [22] c) Raman spectra and vibrational modes assignment for (a) O2-N2 mixture before laser heating, [23] d) Vibration Modes of 'O_2' Isotope shift [24].

IRRAS Geometry in Figure 4 A highlights an electron or incident light IR on the surface of interest at a grazing angle (~ 90°) to maximize absorption, with the reflected beam detected. Any absorption can then be assigned to orbital velocities and vibrational modes of the molecules at the surface, dependent on the polarization of incoming light and the dielectric behavior of the surface.

Figure c) illustrates a mixture of $NO+NO_3^-$ and $NO_2+NO_3^-$ ionic solids after laser heating, measured from high-temperature NO_2 and NO_3 crystals. With similar absorption intensities/cm, previous estimates of O_2 overlap with measured NO_2 asymmetric stretching and O–O bonds, estimated at 1210cm^{-1} peak absorption, with a 28° tilt angle and a 40° calculated θ TDM measured in Ge–O_2 after ORR Ge surface reduction and ATR-IR spectroscopy DTF [23].

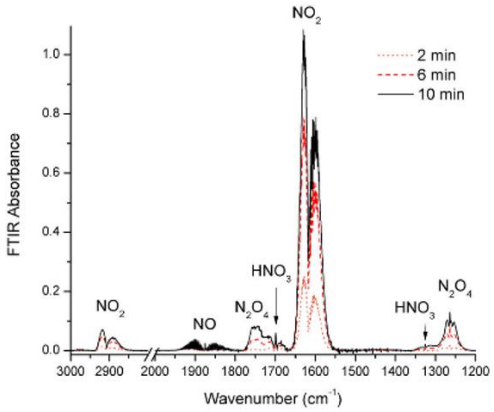

	Vibrational Mode	Wavenumber (cm^{-1})	Specificity
1a	NO_2 wagging	530	TNT
1b	NO_2 symmetric stretching	1350	TNT, RDX,PETN
1c	NO_2 asymmetric stretching	1590	TNT, RDX,PETN
1d	NO_2 symmetric stretching	1390	TNT
2a	CH_3 wagging	460	TNT
2b	CH_3 stretching	760	TNT
3	Ring breathing	1150	TNT
4	$C-C$ stretching	900	RDX
5a	$N-O$ stretching	850-900	PETN
5b	$N-O$ rocking	620	PETN
6	$C-H$ bending	1200,1400	TNT,RDX,PETN
7	$C-O$ stretching	1000 (IR)	PETN
		1160 (Raman)	PETN

Figure 12. Temporal evolution of NO, NO_2, N2O4, and HNO3 in the line of sight of the NOx Box [25]

b) Vibration Modes of Air [26] from Explosives.

With asymmetrical stretch more noticeable in infrared spectrometers, this would correlate to the electron quanta absorbed and emitted. Nitrogen also reacts with hydrogen, oxygen, magnesium, and calcium carbide, and other elements, forming oxides.

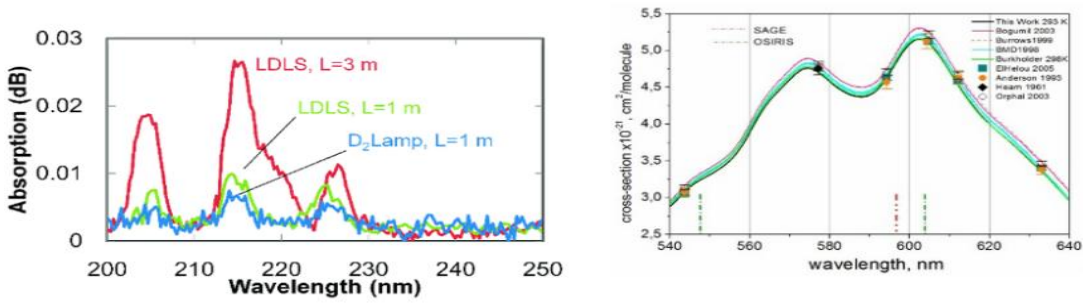

Figure 13. a)Absorption spectra of NO gases (at 1 ppm) from LDLS suggesting 204 nm, 215 nm and 225 nm [27].

In Figure A, the breath analysis system based on UV-absorption spectroscopy, with the main absorbing components in breath being water vapor, isoprene, and ozone [27]. However, other sources suggest alternative absorption and transition methods, such as LCF-WMS spectroscopy for NO and NO_2, to describe emissions in gas turbines with temperature profile fitting [28]. Additionally, absorption of NO derivatives with O_2 is considered [29], and the ozone max Chappuis band, where the green solid is observed, is discussed in [30].

Near/Mid-Infrared Laser Absorption Spectroscopy was used to measure low-absorbance trace NO and NO_2 with strong H_2O interference generated from combustion. Transition lines near 1308 nm, 5238 nm, and 6250 nm were selected to investigate the H_2O, NO, and NO_2 generated from combustion. Ultra-low NOx emissions were captured by optical measurements, and the uncertainty of the TDLAS measurements was analyzed [28]. With measured Absorption transitions within the near-infrared (~1308 nm) and mid-infrared (~6250 nm and ~5238 nm, methods provide accurate detection of low-absorbance NO and NO2 with high H2O interference.

Note: NO absorbs at 1909 and 850-900/cm, with bond stretching and N-O rocking possibly associated with 620/cm and 425-440nm. Smaller NO transitions at 204nm, 215nm, and 225nm correlate to higher energy transitions, indicating greater electron shuffling-mixing absorption in mediums. Regarding the mixing of electrons in N-O sigma and pi bonds, as reflected/refracted electron emission angles approach n°, larger band gaps and non-adjacent shells would cause rocking/stretching vibration modes. This suggests the use of mathematical equations where variables are correlated with nm, which could help characterize variance in observed nm absorption transmission lines in

various mediums and below variables. Since oxygen has one more electron in the p shell at 16 amu than nitrogen, future R&D may utilize infrared spectroscopy, mass spectrometry, and quantify and detect absorption vibration modes $\delta\lambda = \delta v/\delta f$.

For trimolecular configurations such as CO2, there are four vibrational modes: a symmetric stretch, an asymmetric stretch, and two bending modes. The asymmetric stretching mode absorbs at 4.25 μm or 2349 cm^{-1}, while the bending modes absorb at a longer wavelength of 15.0 μm or 667 cm^{-1}. The symmetric mode absorbs at 7.20 μm or 1388 cm^{-1}, as measured by observed Raman spectroscopy. The O-C-O in-plane bending absorbs at 526 cm^{-1}, with illustrations from Purdue University [31].

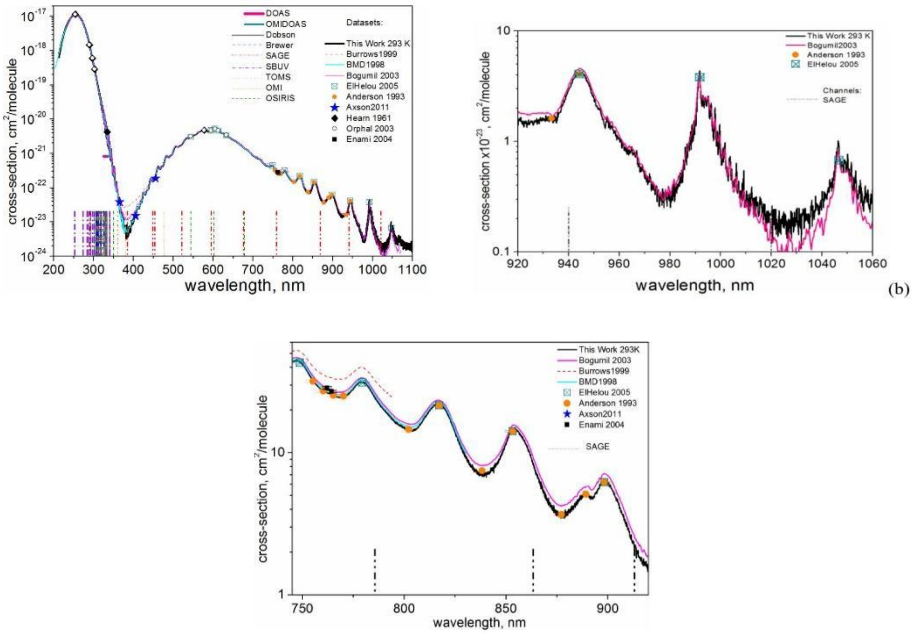

Figure 14. a) Ozone Absorption cross-section at room-temperature, Ozone absorption cross-section datasets in the Wulf band: (a) 750-900 nm, (b) 920-1060 nm [32].

Modern technology, sensors, and data may have difficulty measuring the absorption nm difference between Nitrous oxides (NO_2), N_2O, and O_3. Therefore, misinformation may arise related to substances such as ozone, where NO_2 or O_3 may be present. Measures combining FFT Fourier transform and echelle spectrometers, used by German researchers, have measured air molecules with cross-sections covering 213–1100 nm ± 0.005 nm (2% accuracy), with a spectral resolution of 0.02–0.06 nm in the UV–visible range and 0.12–0.24 nm in the IR at eleven temperatures from 193 to 293K [32]. The spectral resolution mismatch discussed in the Huggins band (320–370 nm, which is UV). Ozone (O_3) measurements from 200–1100 nm consist of four absorption bands: Hartley, Huggins, Chappuis, and Wu.

3.5. NO_2 vs Ozone (O_3) Wavelength Comparison Analysis

Ozone measures peak absorption around 213 nm from Orphal [33], where 250-260 nm collocated with Hartley/Hersberg bands would be more indicative. However, O3 data overlaps with NO measurements from Iwata et al. [27] measured NO at 204 nm, 215 nm, and 225 nm in Figure 13a. Since four orders of magnitude are measured from Orphal [33], this may suggest that higher UV closer to 200 nm is more indicative as an O3 vs. NO2 differentiator, in addition to 350-375 nm measured for NO2. These near-identical nm measurements may suggest both molecules have very similar structures and highlight the challenge of differentiating based on d(nm).

Ozone measured (a) 750-900 nm, (b) 920-1060 nm, and ElHelou [34] measured 945 nm, 990 nm, and 1050 nm for O_3 as highlighted in Figure 14a. Using a tandem dual-beam spectrometer, Anderson [35] and Bogumil [36]

conducted measurements near 1000 nm. However, NO also absorbs at 850-900/cm with bond stretching. For Wu bands, Anderson [35] measured O_3 between 750 and 975 nm at room temperature based on the cross-section method [37]. Ozone also peaks around 550-650 nm [33]; however, NO_2 measured at 530 nm and N-O rocking, associated with 620/cm and 425-440 nm. NO peaks around 425 nm, which would be more indicative of NO. At the maximum of the Chappuis band, green signals from Chappurk [38] and BMD [39] data could differentiate.

While O3 has 18 valence electrons, NO2 has 17 valence electrons, suggesting an unpaired electron. If this indicates higher nm, NO2 absorption peaks could be higher or blue-shifted. However, measuring nm differences in vibration modes with current technology remains a challenge. Additionally, a slight polar bent structure may also contribute to atomic interactions and molecular stability through mixing.

Future R&D may quantitatively differentiate nm or d(nm)/dT. Experiments should utilize the same variable constants, i.e., instrument, environment, time, temperature, pressure, etc., to quantify d(nm) with <5-10nm wavelength spectral accuracy sensitivities.

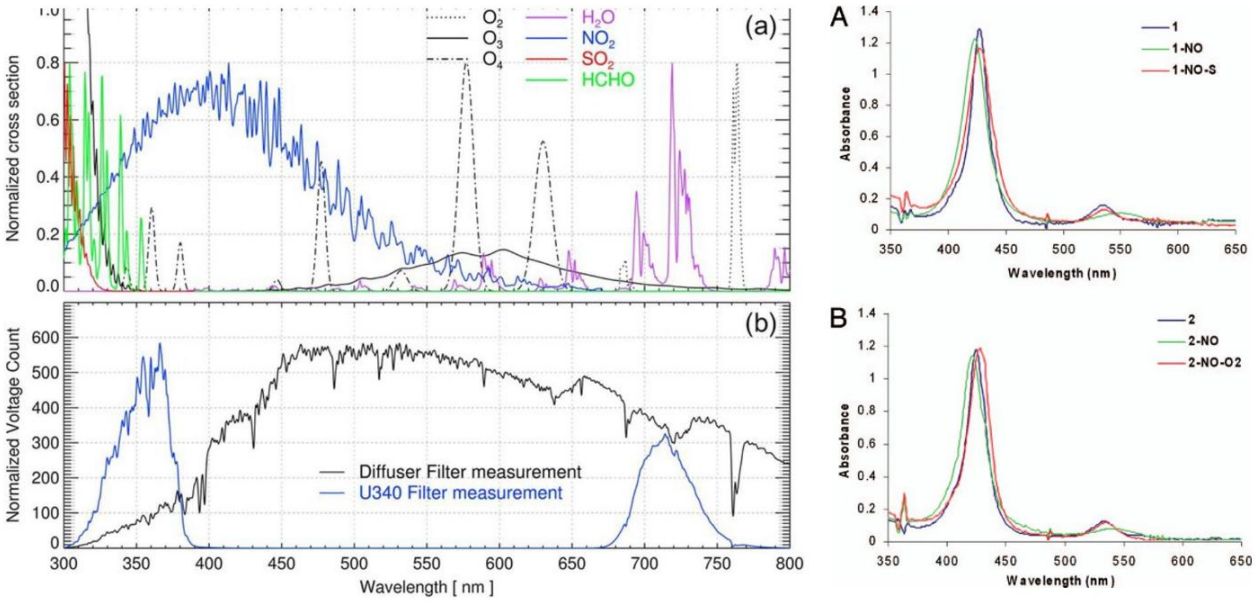

Figure 15. Absorption cross sections of several atmospheric gases convolved with spectral response functions within the spectral range of UV-Vis-NIR spectroradiometer. (b) Mean voltage counts measured with diffuser & U340 filter from 2017 [40] and NO2 from [29].

3.6. Absorption Variance in Data

Modern technology, sensors, and data may have difficulty measuring the absorption nm difference between Nitrous oxides (NO_2 vs N_2O vs O_3). Absorption band lines can change based on Doppler shift, temperature, density, excitation lifetime, vibrational electronic structure, intermolecular interactions, and electromagnetic fields. Higher temperatures lead to more collisions between atoms, which can broaden absorption lines. Higher densities of gas can also broaden absorption lines due to increased pressure and interactions between atoms. The duration an atom spends in an excited state affects the width of the absorption line; a shorter lifetime results in a narrower line. For analyzing absorption spectra in spectroscopy, popular options include SpectraWiz® from StellarNet, ENLIGHTEN™ from Wasatch Photonics, and OPUS from Bruker. These programs often offer data acquisition, peak analysis, and spectral processing.

3.6.1. Air Density, Pressure, Buoyancy Models

Cavendish experiments are the first to analyze atmospheric air and density. The density of air is estimated at 1.19-1.29 grams per liter (g/L) at standard temperature and pressure (STP), which is 25°C (room temperature)

around 101.325 kPa. However, this estimate is based on an atmosphere primarily composed of N2 and O2. An atmosphere of 100% NO2 medium suggests a density of 2.05257 g/L or kg/m^3, indicating that air would be approximately 68% heavier. Based on the formula density = mass/volume, and the ideal gas law density = molar mass / (RT), where R is the gas constant estimated at 0.0821 L·atm/(mol·K), the calculation for NO2 at 25°C (298 K) is: 46.005 / (0.08206 * 273) ≈ 2.05 g/L, assuming the gas constant. This demonstrates how the composition of the atmosphere significantly influences its density, which is crucial for understanding atmospheric behavior and gas interactions in various scientific experiments.

3.6.2. NO In Fuel Cells, Electrolysis, Synthesis, Applications

Nitrogen can also significantly impact fuel cell performance. Nitrogen can permeate the fuel cell membrane and accumulate, particularly at the anode, diluting the fuel (hydrogen) and reducing the cell's efficiency, especially in systems with recirculation. Nitrogen buildup dilutes the hydrogen fuel, reducing the concentration available for the electrochemical reaction at the catalyst sites, which can lead to a drop in voltage and overall performance.

Fuel cells often employ a purging system to periodically vent the accumulated nitrogen. In some fuel cell designs with nitrogen-based fuels, nitrogen is intentionally incorporated into the catalyst material. Nitrogen can bind with metal atoms in catalysts, particularly platinum.

3.7. Nitrogen Oxide Natural and Human Sources

The global Nitrous oxide inventory incorporates both natural and anthropogenic sources and accounts for the interaction between nitrogen additions and the biochemical processes that control Nitrous oxide emissions. Using bottom-up approaches (inventory, statistical extrapolation of flux measurements, process-based land and ocean modelling) and top-down approaches (atmospheric inversion), a comprehensive quantification of global Nitrous oxide sources and sinks has been conducted, covering 21 natural and human sectors between 1980 and 2016. Based on a total of 43 flux estimates, the authors claimed that Nitrous oxide emissions were increasing in emerging economies, including Brazil, China, and India. However, NO flux is also correlated with forest trees.

With nitrogen oxide estimates, atmospheric N_2O increased from 1,462 Tg N in the 1980s to 1,555 Tg N in 2007–2016, with a possible uncertainty of ±20 Tg N. 'Natural soil baseline' emissions were obtained from six terrestrial biosphere models such as the Global N_2O Model Intercomparison Project (NMIP) [41] and were compared with three global inventories (FAOSTAT, EDGAR v4.3.2, and GAINS). With a new category from 'Lightning and atmospheric production,' regional observations of low oxygen ocean zones have also suggested that these regions may produce more nitrogen oxide than is simulated by the models [42]. If NOx is lost or denitrification occurs, this is claimed to delay deactivation of charge state ions and extend ozone depletion throughout the winter and early spring. This suggests that nitrogen oxides (NO_2 vs N_2O vs O_3) neutralize reactive species and reduce ozone destruction, which would play an important role in maintaining atmospheres, electromagnetic fields, and regulating heat to prevent ice melting in Earth's polar regions.

4. DISCUSSION

Data and R&D on both material abiotic, cells, biology, oxides studied since the 1970s suggest N-O mixing ratios and that atmospheres and planets have a preference for polar bent and tri-molecular structures such as NO_2 and H_2O. Modern technology, sensors, and data may have difficulty measuring the differences between Nitrous oxide (N_2O), NO_2, and O_3. There are sources of misinformation around nitrous oxides and their respective absorption/emission spectra, profiles, or productions, as well as sources colocated with Negative Air Ions (NAIs). This could impact various industries, technologies, and applications, including oxide redox reactions, medical and biological fields, thermal decomposition, high-temperature corrosion, and vehicle emissions, all of which influence chemical reaction pathways.

4.1. Nitric Acids, Safety

Nitrous oxide has many medical uses, such as pain-reducing effects. After English chemist Humphry Davy's work in the early 1800s, recreational use of nitrous oxide became popular among the British upper class as "laughing gas." Philosopher Joseph Priestley described producing "nitrous airs" after heating iron filings soaked in nitric acid. In a 1775 publication, Priestley proposed to have discovered oxygen (c. 1774). In 1798, such nitrous oxides were produced in quantity to treat patients with a range of lung diseases and others. In 1800, he noted the analgesic effect and potential surgical uses of N_2O or NO_2. Although some claims suggest side effects of prolonged consumption, including headaches, nausea, and vomiting, which could be associated with heavy metals. Laughing gas in modern day is produced from thermal decomposition of ammonium nitrate $NH_4NO_3 \rightarrow N_2O + 2\ H_2O$, which is produced by reacting ammonia gas with nitric acid. Nitric acid (HNO_3) can be generated when ammonia is oxidized with air, such as $NH_3 + NO_2 \rightarrow NO + H_2O + O_n$.

If some claim that NO_2 is not safe to inhale, this could be correlated to high temperature corrosion (HTC) and vehicle exhaust emissions colocated with high charge state metals. If quantifying measuring NO_2 vs Al_nO_n, Fe_nO_n oxides from combustion is overlooked, NO_2 data online currently could be correlated with misinformation.

4.2. Nitrogen Oxides, NO and NO_2 in Biology and Amino Acids

Moreover, NO and NO_2 are the most abundant nitrogen molecules synthesized by many cells [43] that diffuse rapidly in cells. Moreover, NO synthase enzyme is also believed to emit the gaseous hormone NO [29]. As nitrogen can diffuse through the lungs, cells can further regulate nitrogen flow through nitrogen dioxide (NO_2) diffusion, which is largely unimpeded by cell membranes [44].

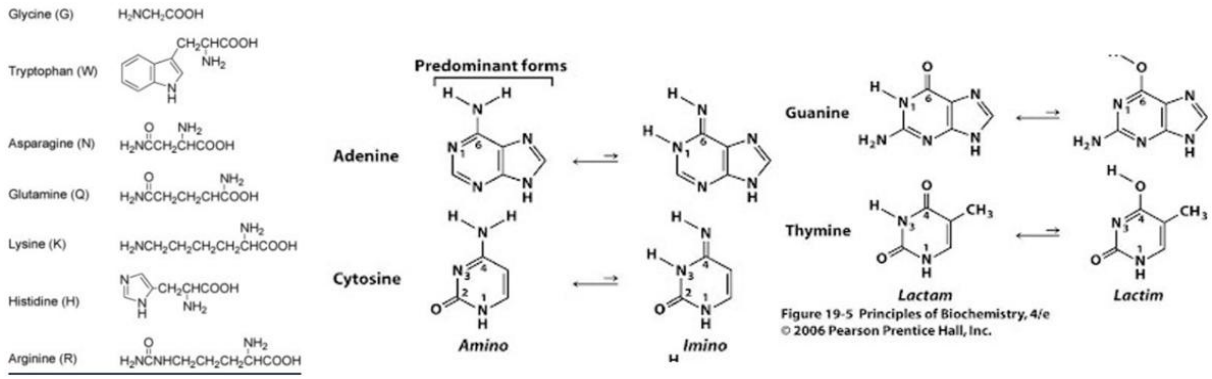

Figure 16. Aminos with N-O bonds application of nitrogen-rich amino acids [45].

5. CONCLUSIONS

Based on data collected by balloons and satellites since the 1980s, data suggests Earth atmospheres have a preference for trimolecules such as NO_2 and polar bent molecular structures, similar to H_2O. Flight data indicates that the column data for NO and NO_2 estimates a ratio of $3NO_2$: 1NO and $4NO_2$: 1NO near the surface, which is similar to the proposed 78% "N_2 measurements." Measurements of 1NO: 2-6 NO_2 have been recorded at altitudes of 10-12 km from Shah et al. [17], although no N_2 data has been documented. Atmospheric nitrous oxide increased from 1,462 Tg N in the 1980s to 1,555 Tg N during 2007–2016, according to the Global Model Intercomparison Project (NMIP) [41], which compared data with three global models (FAOSTAT, EDGAR v4.3.2, and GAINS). Data suggests that NO and NO_2 are the most abundant nitrogen molecules synthesized by many cells. With NO_2 and NO as primary atmospheric constituents, this research holds significant potential to improve Earth and atmospheric sciences, climate studies, and various systems including energy, fuel cells, combustion, redox surface reactions, planetary science, astronomy, and models across the Universe.

Funding: This study received no specific financial support.
Institutional Review Board Statement: Not applicable.
Transparency: The author states that the manuscript is honest, truthful, and transparent, that no key aspects of the investigation have been omitted, and that any differences from the study as planned have been clarified. This study followed all writing ethics.
Competing Interests: The author declares that there are no conflicts of interests regarding the publication of this paper.

REFERENCES

[1] J. B. West, "Henry Cavendish (1731–1810): Hydrogen, carbon dioxide, water, and weighing the world," *American Journal of Physiology-Lung Cellular and Molecular Physiology*, vol. 307, no. 1, pp. L1-L6, 2014. https://doi.org/10.1152/ajplung.00067.2014

[2] J. Labidi *et al.*, "Hydrothermal 15N15N Abundances Constrain the Origins of Mantle Nitrogen," *Nature*, vol. 580, no. 7803, pp. 367-371, 2020. https://doi.org/10.1038/s41586-020-2173-4

[3] T. Mather, A. Allen, B. Davison, D. Pyle, C. Oppenheimer, and A. McGonigle, "Nitric acid from volcanoes," *Earth and Planetary Science Letters*, vol. 218, no. 1-2, pp. 17-30, 2004. https://doi.org/10.1016/S0012-821X(03)00640-X

[4] R. Sánchez-Gutiérrez *et al.*, "Nitrate legacy in a tropical and complex fractured volcanic aquifer system," *Journal of Geophysical Research: Biogeosciences*, vol. 128, no. 8, p. e2023JG007554, 2023. https://doi.org/10.1029/2023JG007554

[5] Y. Guo *et al.*, "A SARS-CoV-2 neutralizing antibody with extensive Spike binding coverage and modified for optimal therapeutic outcomes," *Nature Communications*, vol. 12, no. 1, p. 2623, 2021. https://doi.org/10.1038/s41467-021-22926-2

[6] C. Ye *et al.*, "Rapid cycling of reactive nitrogen in the marine boundary layer," *Nature*, vol. 532, no. 7600, pp. 489-491, 2016. https://doi.org/10.1038/nature17195

[7] C. Reed, M. J. Evans, P. Di Carlo, J. D. Lee, and L. J. Carpenter, "Interferences in photolytic NO 2 measurements: Explanation for an apparent missing oxidant?," *Atmospheric Chemistry and Physics*, vol. 16, no. 7, pp. 4707-4724, 2016. https://doi.org/10.5194/acp-16-4707-2016

[8] P. Kasibhatla *et al.*, "Global impact of nitrate photolysis in sea-salt aerosol on NO x, OH, and O 3 in the marine boundary layer," *Atmospheric Chemistry and Physics*, vol. 18, no. 15, pp. 11185-11203, 2018. https://doi.org/10.5194/acp-18-11185-2018

[9] S. T. Andersen *et al.*, "Extensive field evidence for the release of HONO from the photolysis of nitrate aerosols," *Science Advances*, vol. 9, no. 3, p. eadd6266, 2023. https://doi.org/10.1126/sciadv.add6266

[10] J. A. Fisher *et al.*, "Methyl, ethyl, and propyl nitrates: Global distribution and impacts on reactive nitrogen in remote marine environments," *Journal of Geophysical Research: Atmospheres*, vol. 123, no. 21, pp. 12,429-12,451, 2018. https://doi.org/10.1029/2018JD029046

[11] D. Camuffo, "Theoretical grounds for humidity. In D. Camuffo (Ed.), Microclimate for cultural heritage," 2nd ed. Amsterdam, Netherlands: Elsevier, 2014, pp. 49–76.

[12] P. Jensen, M. Spanner, and P. Bunker, "The CO2 molecule is never linear," *Journal of Molecular Structure*, vol. 1212, p. 128087, 2020. https://doi.org/10.1016/j.molstruc.2020.128087

[13] M. J. Jafari, "Application of vibrational spectroscopy in organic electronics," Doctoral Dissertation, Linköping University Electronic Press, 2017.

[14] W. Junkermann and T. Ibusuki, "FTIR spectroscopic measurements of surface bond products of nitrogen oxides on aerosol surfaces—implications for heterogeneous HNO2 production," *Atmospheric Environment. Part A. General Topics*, vol. 26, no. 17, pp. 3099-3103, 1992. https://doi.org/10.1016/0960-1686(92)90466-X

[15] Y. Kondo, "Reactive nitrogen (NOx and NOy). In G. R. North, J. Pyle, & F. Zhang (Eds.), Encyclopedia of Atmospheric Sciences," 2nd ed. United Kingdom: Academic Press, 2015, pp. 242–249.

[16] B. A. Ridley, M. A. Carroll, and G. L. Gregory, "Measurements of nitric oxide in the boundary layer and free troposphere over the Pacific Ocean," *Journal of Geophysical Research: Atmospheres*, vol. 92, no. D2, pp. 2025-2047, 1987. https://doi.org/10.1029/JD092iD02p02025

[17] V. Shah *et al.*, "Nitrogen oxides in the free troposphere: implications for tropospheric oxidants and the interpretation of satellite NO 2 measurements," *Atmospheric Chemistry and Physics*, vol. 23, no. 2, pp. 1227-1257, 2023. https://doi.org/10.5194/acp-23-1227-2023

[18] L. Yu, Y. Zhang, L. Wang, X. Liu, Y. Zhang, and F. Li, "Regional and temporal variations of tropospheric NO_2 and their relationship with air quality models," *Journal of Atmospheric Science*, vol. 73, no. 5, pp. 1482-1495, 2016.

[19] S. Wang *et al.*, "Solar 11-year cycle signal in stratospheric nitrogen dioxide—Similarities and discrepancies between model and NDACC observations," *Solar Physics*, vol. 295, p. 117, 2020. https://doi.org/10.1007/s11207-020-01685-1

[20] K. F. Boersma *et al.*, "Near-real time retrieval of tropospheric NO_2 from OMI," *Atmospheric Chemistry and Physics*, vol. 7, pp. 2103–2118, 2007. https://doi.org/10.5194/acp-7-2103-2007

[21] C. Xu, N. Huret, M. Garnung, and S. Celestin, "A new detailed plasma-chemistry model for the potential impact of blue jet streamers on atmospheric chemistry," *Journal of Geophysical Research: Atmospheres*, vol. 125, no. 6, p. e2019JD031789, 2020. https://doi.org/10.1029/2019JD031789

[22] R. Moreh, Y. Finkelstein, and D. Nemirovsky, "Nuclear resonance photon scattering studies of N2 adsorbed on Grafoil and of NaNO2 Single Crystal," *Journal of Research of the National Institute of Standards and Technology*, vol. 105, no. 1, pp. 159-166, 2000. http://dx.doi.org/10.6028/jres.105.022

[23] A. Y. Kuznetsov, L. Dubrovinsky, A. Kurnosov, M. Lucchese, W. Crichton, and C. Achete, "High-Pressure Synthesis and Study of NO+ NO 3− and NO 2+ NO 3− Ionic Solids," *Advances in Physical Chemistry*, vol. 2009, no. 1, p. 180784, 2009. https://doi.org/10.1155/2009/180784

[24] S. Nayak, P. U. Biedermann, M. Stratmann, and A. Erbe, "A mechanistic study of the electrochemical oxygen reduction on the model semiconductor n-Ge (100) by ATR-IR and DFT," *Physical Chemistry Chemical Physics*, vol. 15, no. 16, pp. 5771-5781, 2013. http://dx.doi.org/10.1039/c2cp43909c

[25] M. Pavlovich *et al.*, "Air spark-like plasma source for antimicrobial NOx generation," *Journal of Physics D: Applied Physics*, vol. 47, no. 50, p. 505202, 2014. http://dx.doi.org/10.1088/0022-3727/47/50/505202

[26] E. Finot, T. Brulé, P. Rai, A. Griffart, A. Bouhélier, and T. Thundat, "Raman and photothermal spectroscopies for explosive detection. In Micro- and Nanotechnology Sensors, Systems, and Applications V," vol. 8725. United States: SPIE, 2013, pp. 437–448.

[27] T. Iwata, T. Katagiri, and Y. Matsuura, "Real-time analysis of isoprene in breath by using ultraviolet-absorption spectroscopy with a hollow optical fiber gas cell," *Sensors*, vol. 16, no. 12, p. 2058, 2016. https://doi.org/10.3390/s16122058

[28] J. Li *et al.*, "In situ measurement of NO, NO2, and H2O in combustion gases based on near/mid-infrared laser absorption spectroscopy," *Sensors*, vol. 22, no. 15, p. 5729, 2022. https://doi.org/10.3390/s22155729

[29] J. P. Collman *et al.*, "Interaction of nitric oxide with a functional model of cytochrome c oxidase," *Proceedings of the National Academy of Sciences*, vol. 105, no. 29, pp. 9892-9896, 2008. https://doi.org/10.1073/pnas.0804257105

[30] J. B. Burkholder and R. K. Talukdar, "Temperature dependence of the ozone absorption spectrum over the wavelength range 410 to 760 nm," *Geophysical Research Letters*, vol. 21, no. 7, pp. 581–584, 1994. https://doi.org/10.1029/93GL02311

[31] Purdue University, *Illustrations and vibrational modes of CO_2*. West Lafayette, IN: Purdue University, Department of Chemistry, 2025.

[32] V. Gorshelev, A. Serdyuchenko, M. Weber, W. Chehade, and J. Burrows, "High spectral resolution ozone absorption cross-sections–Part 1: Measurements, data analysis and comparison with previous measurements around 293 K," *Atmospheric Measurement Techniques*, vol. 7, no. 2, pp. 609-624, 2014. https://doi.org/10.5194/amt-7-609-2014

[33] J. Orphal, "A critical review of the absorption cross-sections of O3 and NO2 in the ultraviolet and visible," *Journal of Photochemistry and Photobiology A: Chemistry*, vol. 157, no. 2–3, pp. 185–209, 2003. https://doi.org/10.1016/S1010-6030(03)00061-3

[34] M. ElHelou, "Ozone measurement methods and applications," *Atmospheric Chemistry Research*, vol. 19, no. 4, pp. 672-678, 2005.

[35] T. A. Anderson, "Dual beam spectrometry for ozone measurements," *Atmospheric Spectroscopy*, vol. 2, no. 3, pp. 138-143, 1993.

[36] K. Bogumil, "Ozone measurements in the spectral region near 1000 nm," *Atmospheric Measurement Techniques*, vol. 10, no. 2, pp. 415-421, 2003.

[37] S. M. Anderson, P. Hupalo, and K. Mauersberger, "Ozone absorption cross section measurements in the Wulf bands," *Geophysical Research Letters*, vol. 20, no. 15, pp. 1579-1582, 1993. https://doi.org/10.1029/93GL01765

[38] T. Chappurk, "Ozone absorption spectra and their relation to NO and NO_2," *Spectroscopy Journal*, vol. 35, no. 9, pp. 311-317, 1994.

[39] BMD, "Ozone absorption spectra: A comparison between O_3 and NO measurements," *Atmospheric Chemistry and Physics*, vol. 12, no. 2, pp. 234-239, 1998.

[40] U. Jeong *et al.*, "Langley calibration analysis of solar spectroradiometric measurements: Spectral aerosol optical thickness retrievals," *Journal of Geophysical Research: Atmospheres*, vol. 123, no. 8, pp. 4221-4238, 2018. https://doi.org/10.1002/2017JD028262

[41] H. Tian *et al.*, "Global soil nitrous oxide emissions since the preindustrial era estimated by an ensemble of terrestrial biosphere models: Magnitude, attribution, and uncertainty," *Global Change Biology*, vol. 25, no. 2, pp. 640-659, 2019. https://doi.org/10.1111/gcb.14514

[42] M. Manizza, R. F. Keeling, and C. D. Nevison, "On the processes controlling the seasonal cycles of the air–sea fluxes of O2 and N2O: A modelling study," *Tellus B: Chemical and Physical Meteorology*, vol. 64, no. 1, p. 18429, 2012. https://doi.org/10.3402/tellusb.v64i0.18429

[43] M. C. Martínez and R. Andriantsitohaina, "Reactive nitrogen species: Molecular mechanisms and potential significance in health and disease," *Antioxidants & Redox Signaling*, vol. 11, no. 3, pp. 669–702, 2009. https://doi.org/10.1089/ars.2007.1993

[44] M. N. Møller, E. Cuevasanta, F. Orrico, A. C. Lopez, L. Thomson, and A. Denicola, *Diffusion and transport of reactive species across cell membranes. In A. Trostchansky & H. Rubbo (Eds.), Bioactive lipids in health and disease (Advances in Experimental Medicine and Biology*. Cham: Springer, 2019.

[45] J. Maruyama, N. Fukui, M. Kawaguchi, and I. Abe, "Application of nitrogen-rich amino acids to active site generation in oxygen reduction catalyst," *Journal of Power Sources*, vol. 182, no. 2, pp. 489-495, 2008. https://doi.org/10.1016/j.jpowsour.2008.04.040